Electronic Supplementary Material (ESI) for Inorganic Chemistry Frontiers.

High-Efficiency Tunable Self-Trapped Emission in One-Dimensional β-$Cs_3Cu_2Br_5$ via Ag Alloying for Optoelectronic Application

Xin Xu,[a] Zhongyi Wang,[a] Qingkun Kong,[b] Siping Liu,[c] Ruiling Zhang, [a] Xiaojing Liu*, [a] and Keli Han.[a,d]*

[a] Institute of Frontier Chemistry, School of Chemistry and Chemical Engineering, Shandong University, Qingdao, 266237, P.R. China.

[b] Key Laboratory of Catalytic Conversion and Clean Energy in Universities of Shandong Province, School of Chemistry and Chemical Engineering, Qufu Normal University, Qufu 273165, P. R. China.

[c] Guangxi Key Laboratory of Chemistry and Engineering of Forest Products, School of Chemistry and Chemical Engineering, Guangxi Minzu University, Nanning 530006, P. R. China.

[d] State Key Laboratory of Molecular Reaction Dynamics, Dalian Institute of Chemical Physics, Chinese Academy of Science, Dalian 116023, P.R.China.

Corresponding Author

Xiaojing Liu*, E-mail: liuxj2020@sdu.edu.cn; Ruiling Zhang*, E-mail: rlzhang@sdu.edu.cn.

Experimental Section

Materials

Cesium bromide (CsBr, 99.99%), Silver bromide (AgBr, 99.99%), Hydrobromic acid (HBr, 48 wt.% in H_2O) and Hypophoaphoeous acid (H_3PO_2, 50 wt.% in H_2O) was purchased from Shanghai Aladdin Biochemical Technology Co., Ltd. Cuprous bromide (CuBr, 99.99%) was bought from TCI Shanghai Chemicals Industry Co., Ltd. All of the chemicals were used without further purifications.

Synthesis of $Cs_3Cu_2Br_5$ Single Crystals

1.0 mmol CsBr, 0.25 mmol CuBr was added to 5 mL glass vial. 1.0 mL HBr and 0.2 mL H_3PO_2 was then added. The mixture was heated to 165 ℃ on a hot plate for 30 min to dissolve the powders. Blue-emissive crystals were yielded after naturally cooling the solutions at ambient conditions, while the needle-like cyan-emissive crystals were yield after rapidly cooling down the hot solutions. The needle-like cyan-emissive crystals were unstable in ambient conditions.

Synthesis of Ag-alloyed $Cs_3Cu_2Br_5$ Single Crystals

To synthesize Ag-alloyed $Cs_3Cu_2Br_5$ single crystals, 1.0 mmol CsBr, 0.25 mmol CuBr and x mg (x = 5, 10, 20, 30 and 40 mg) was added to 5 mL glass vial. 1.0 mL HBr and 0.2 mL H_3PO_2 was then added. The mixture was heated to 165 ℃ on a hot plate for 30 min to dissolve the powders. Colorless crystals were yielded after naturally cooling at ambient conditions, the synthesized crystals were named as β-$Cs_3Cu_2Br_5$:xAg^+ (x = 6.52%, 12.40%, 17.32%, 20.56% and 32.35%.). The

product with addtion of 5 mg Ag is unstable and will transform to 0D blue emissive $Cs_3Cu_2Br_5$ within seveal minutes in solutions.

Characterization

Powder X-ray diffraction (XRD) measurements were performed on a Rigaku smartlab9kw diffractometer equipped with Cu Kα radiation. Room-temperature photoluminescence (PL), time-resolved PL, temperature-dependent PL spectra were recorded on the FLS 1000 Edinburgh Instruments spectrofluorimeter equipped with a xenon lamp as the excitation source. Single Crystal X-ray diffraction (SCXRD) results were acqiured by Rigaku Oxford XtaLAB Synergy-DW diffractometer with monochromated Mo Kα radiation (λ = 0.7107 Å). X-ray photoelectron spectroscopy (XPS) measurements were performed by using Thermofisher ESCALAB Xi+ with the X-ray source of monochromated Al Kα (hv = 1486.6eV). The absolute quantum yield was measured by Hamamatsu C9920-02 equipped with integrating sphere. Femtosecond transient absorption (fs TA) measurements were performed by a pump-probe laser system (800 nm, 50 fs, and 1 kHz repetition rate) based on a regenerative amplified Ti:sapphire laser source (Spectra Physics). The sample was excited by 340 nm laser pulses generated by a TOPAS Optical Parametric Amplifier (OPA) which was pumped by the 800 nm pulse. A white light continuum (WLC) generated by a 2 mm thick CaF_2 was used as the probe beam. The excitation energy is 44 μw.

***Calculation of tetrahedral parameters*:**

Tetrahedral parameters of Δd and σ^2 was calculated by the following equations.[1, 2]

$$\Delta d = \frac{1}{4}\sum_{n=1}^{4}\left(\frac{d_n - d}{d}\right)^2$$

$$\sigma^2 = \frac{1}{5}\sum_{n=1}^{6}\left(\theta_n - 109.47°\right)^2$$

In the above equations, d_n and d represents the individual bond length and average bond length in $[CuBr_4]^{3-}$ tetrahedron; θ_n is the specific Br-Cu-Br bond angle and average in $[CuBr_4]^{3-}$ tetrahedron. Δd describes the overall tetrahedral elongation and variation in tetrahedral bond distance, and the variation and deviation of bond angle in $[CuBr_4]^{3-}$ tetrahedron could be reflected by σ^2. Taking these two parameters into consideration, the distortion of 1D Ag-alloyed β-$Cs_3Cu_2Br_5$ crystal lattice induced by temperature and Ag ion can be correctly determined.

Computational methods

The DFT calculations were performed on Vienna ab initio Simulation package (VASP) [3, 4] with projector augmented wave (PAW) pseudopotential.[5, 6] The exchange-correlation interaction was described by Perdew-Burke-Ernzerhof (PBE) functional within the generalized gradient approximation (GGA).[7, 8] The kinetic energy cut-off was set to 400 eV. The Brillouin zone was sampled by Gamma-centered (Monkhorst–Pack) k-point with 2 × 3 × 3. The convergence criterion of force and energy were set to 0.01 eV $Å^{-1}$ and 10^{-5} eV, respectively.[9, 10]

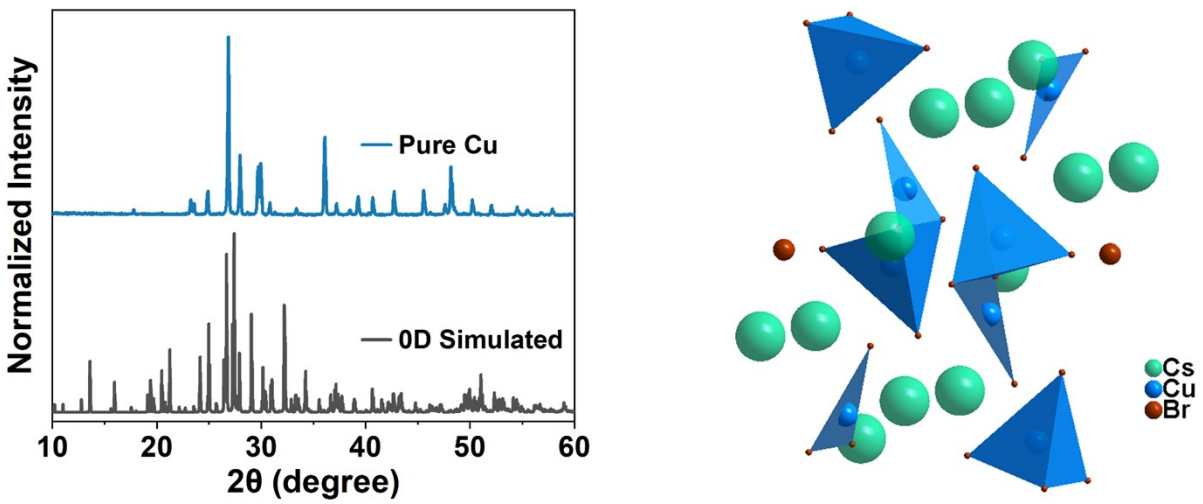

Fig. S1 PXRD patterns of blue-emissive copper bromide crystals, and the crystal strucutre of 0D $Cs_3Cu_2Br_5$.

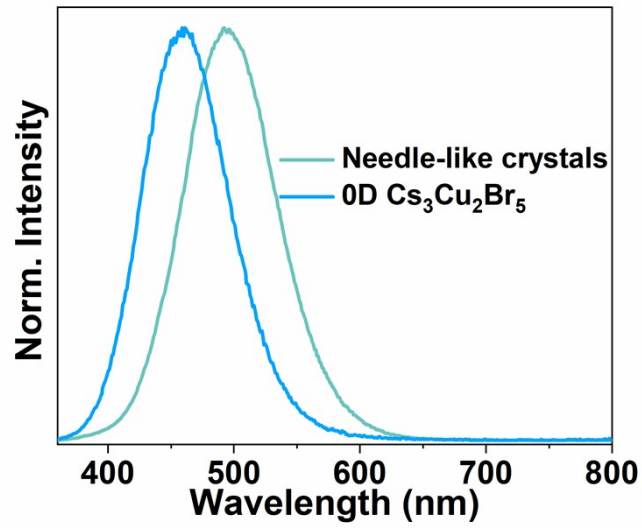

Fig. S2 PL spectra of 0D $Cs_3Cu_2Br_5$ and needle-like crystals.

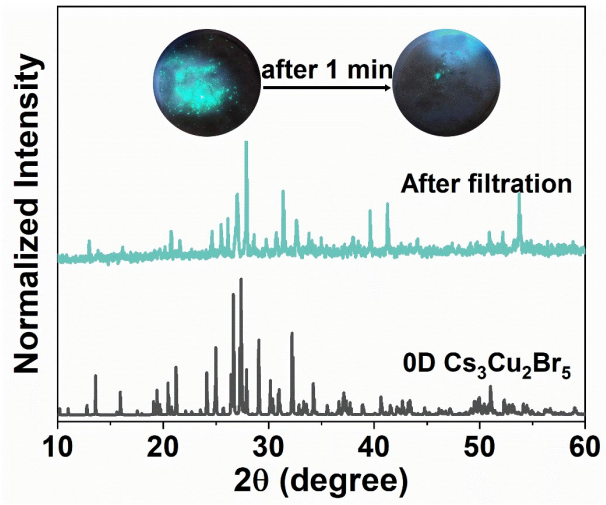

Fig. S3 PXRD patterns of needle-shape copper bromide crystals after filtration.

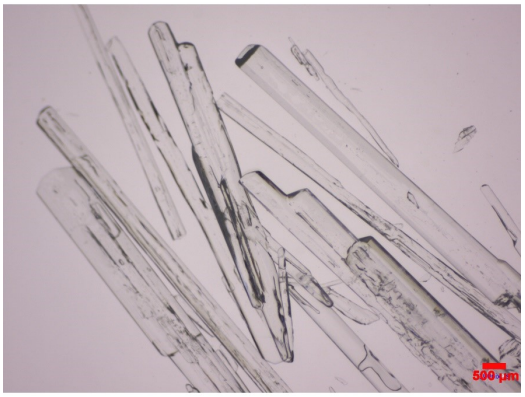

Fig. S4 Photograph of the synthisized 1D $Cs_3(Cu/Ag)_2Br_5$ crystal under optical microscope.

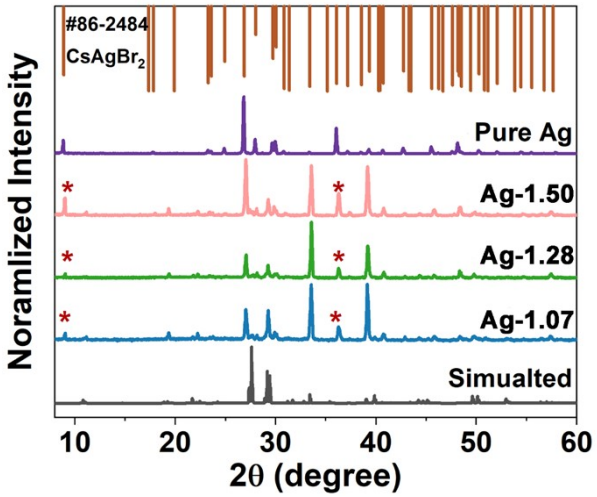

Fig. S5 PXRD patterns of Ag-1.07, Ag-1.28, Ag-1.50 and pure Cesuim silver bromide crystals. (The asterisks represent the $CsAgBr_2$ impurities, 1.07, 1.28 and 1.50 represents the Ag/Cu feeding ratio.)

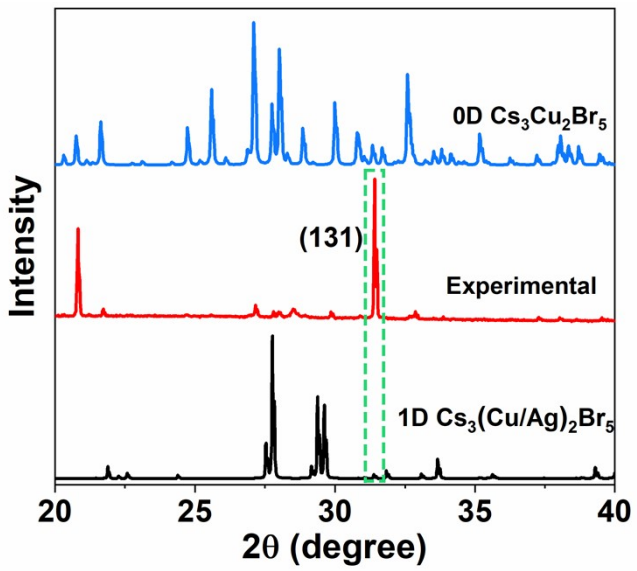

Fig. S6 The comparison of the PXRD patterns of needle-like crystals, 1D $Cs_3(Cu/Ag)_2Br_5$ and 0D $Cs_3Cu_2Br_5$.

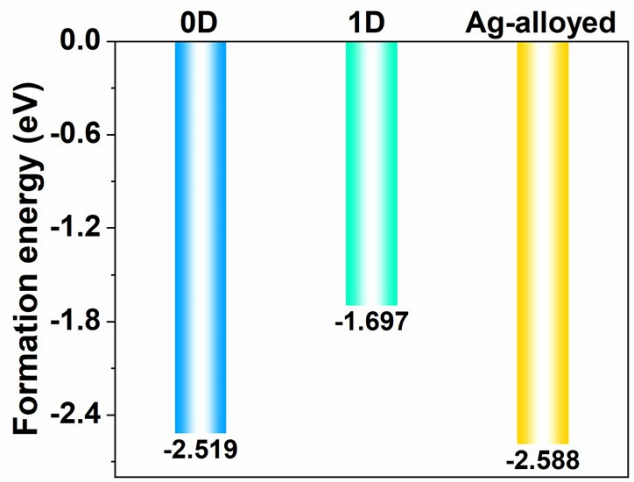

Fig. S7 Formation energy of 0D $Cs_3Cu_2Br_5$, 1D β-$Cs_3Cu_2Br_5$ and Ag-alloyed β-$Cs_3Cu_2Br_5$ (Slected β-$Cs_3Cu_2Br_5$:32.35%Ag^+ as model). The formation energies are calculated with respect to the precursors CsBr, CuBr and AgBr, as $E_f = E[Cs_3Cu_2Br_5] - 3E[CsBr] - 2E[CuBr]$, where E is the total energy. Calculations are performed at 0 K and 0 Gpa.

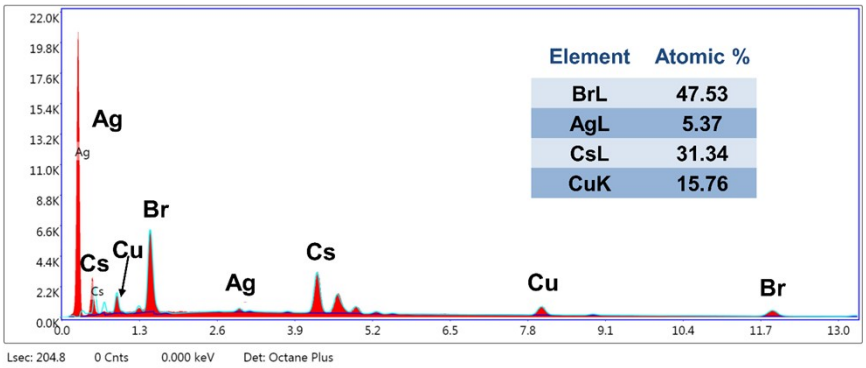

Fig. S8 EDS results of β-$Cs_3Cu_2Br_5$:20.56%Ag^+, and the inset table shows the estimated atom ratio of Cs, Ag, Cu and Br, respectively.

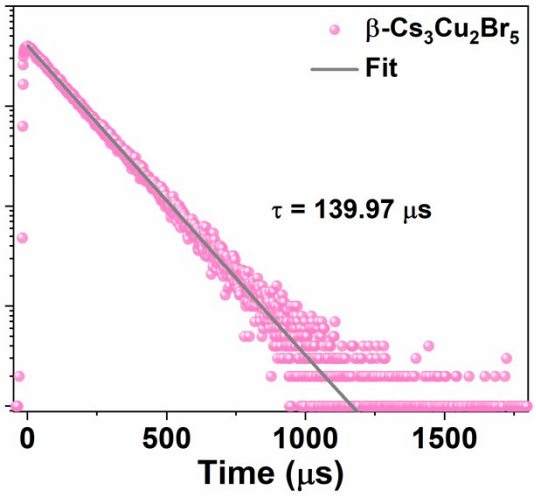

Fig. S9 PL decay curve of 1D β-$Cs_3Cu_2Br_5$ sample at room temperature.

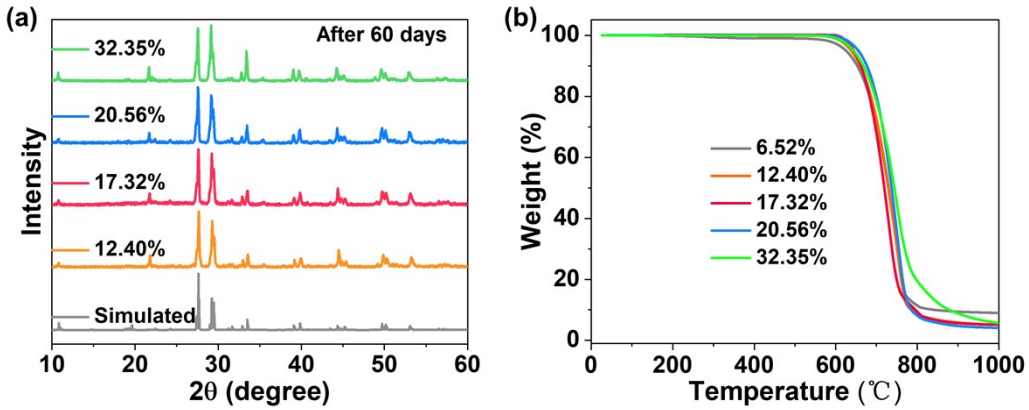

Fig. S10 (a) PXRD patterns of Ag-alloyed β-$Cs_3Cu_2Br_5$ samples after storing at ambient conditions for 60 days. (b) thermogravimetric analysis of Ag-alloyed β-$Cs_3Cu_2Br_5$ samples.

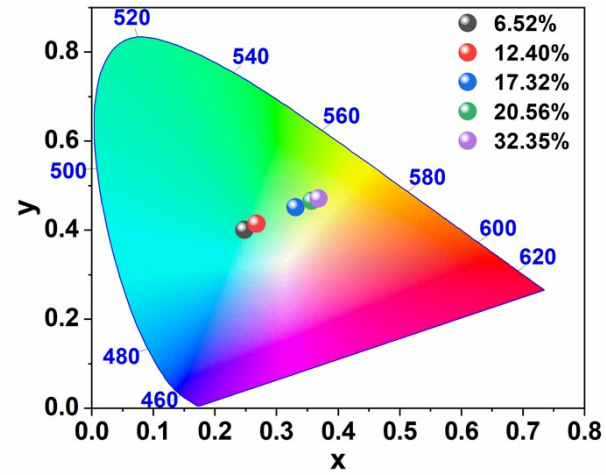

Fig. S11 CIE color coordinates of β-$Cs_3Cu_2Br_5$:xAg.

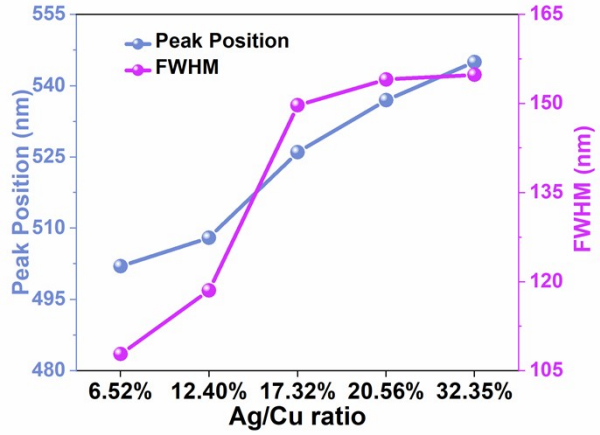

Fig. S12 Peak positions and FWHM of Ag-alloyed β-$Cs_3Cu_2Br_5$.

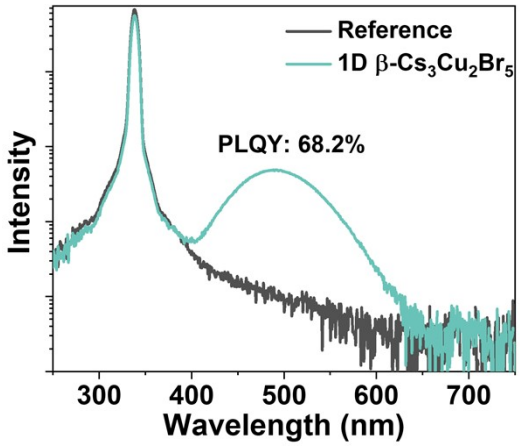

Fig. S13 PLQY of 1D β-$Cs_3Cu_2Br_5$.

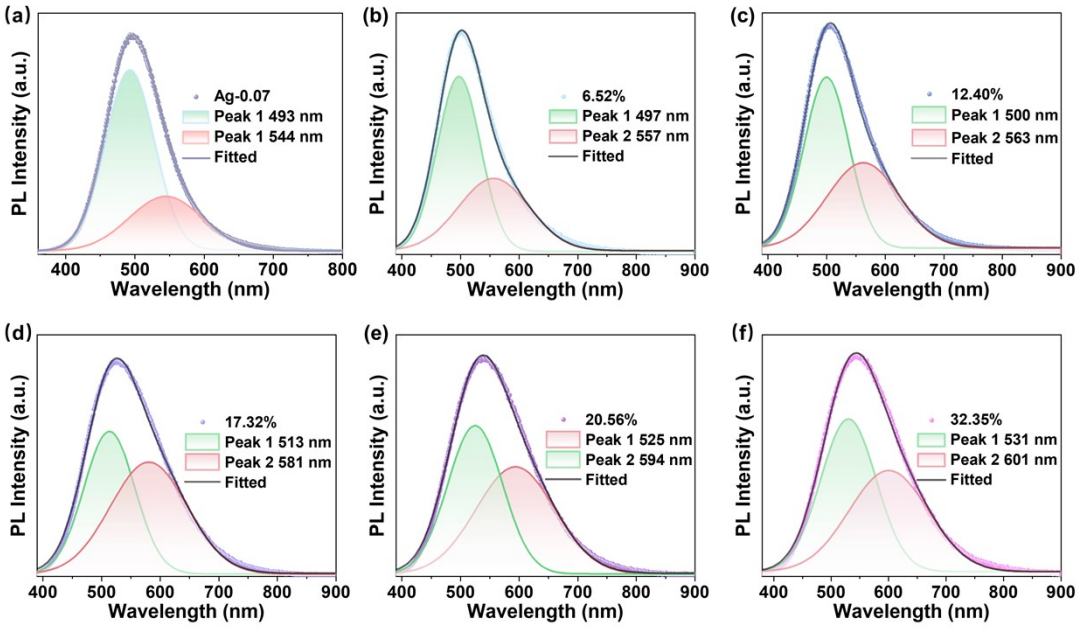

Fig. S14 PL spectra of β-$Cs_3Cu_2Br_5$:xAg^+ with fitting by two Gaussian distributions, peak 1 and peak 2 (Note: In Fig.S13a, 0.07 represents the feeding Ag/Cu ratio.).

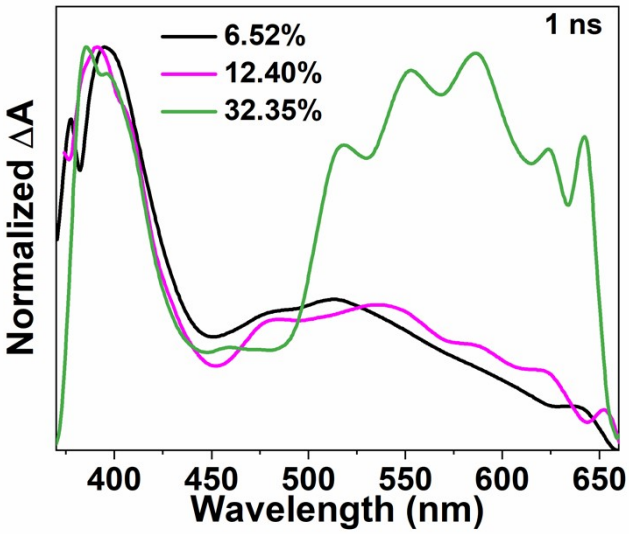

Fig. S15 The fs-TA spectra of β-$Cs_3Cu_2Br_5$:xAg^+ (x= 6.52%, 12.40% and 32.35%) at the detection time of 1 ns.

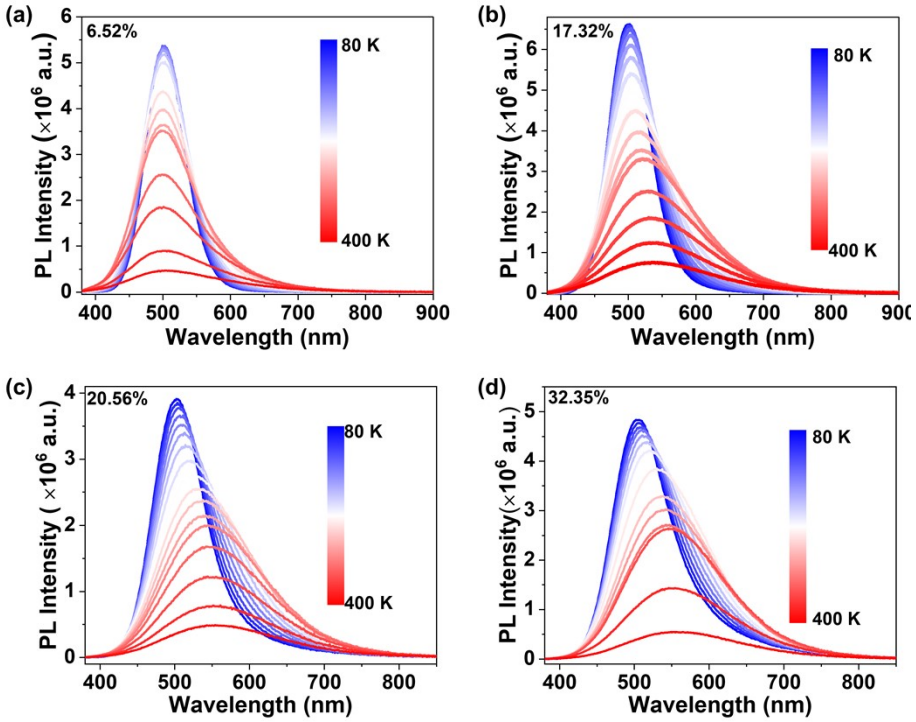

Fig. S16 Temperature-dependent PL spectra of β-$Cs_3Cu_2Br_5$:xAg^+ (x= 6.52%, 17.32%, 20.56% and 32.35%) samples

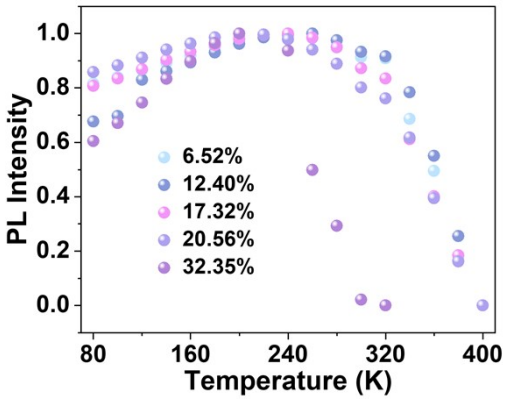

Fig. S17 Temperature-dependent PL intensity of β-$Cs_3Cu_2Br_5$:xAg^+ (x= 6.52%, 12.40%, 17.32%, 20.56% and 32.35%) samples

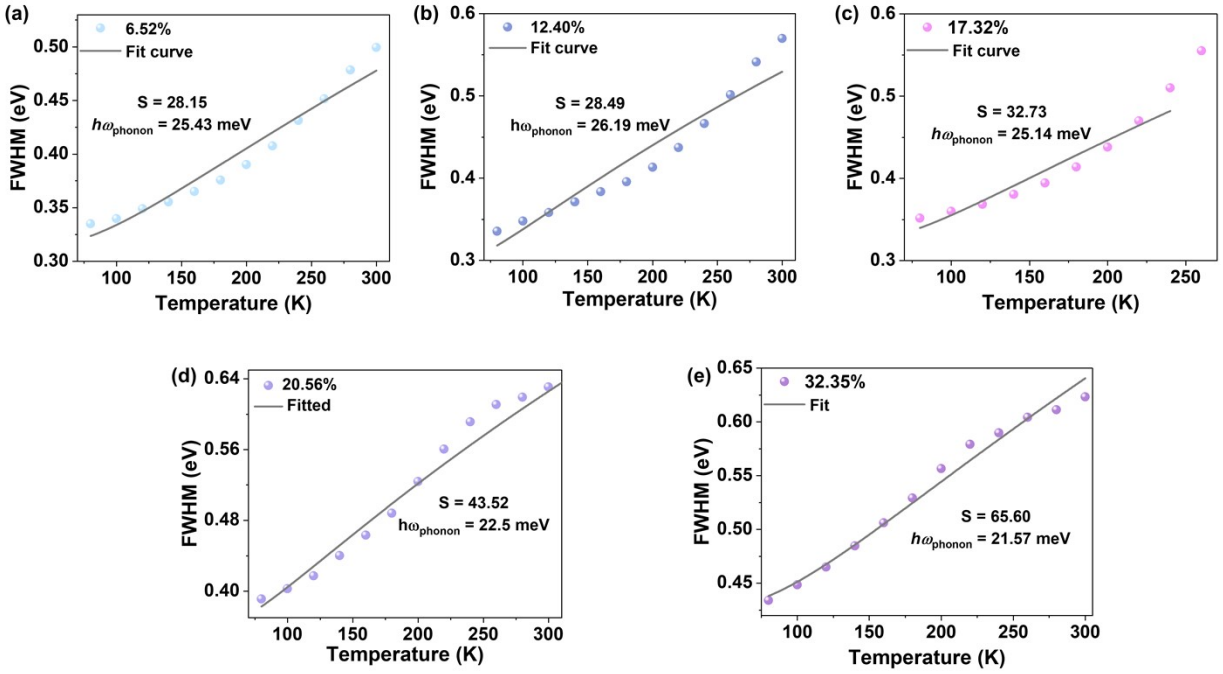

Fig. S18 Temperature-dependent FWHM and fitting curves.

Note. Huang-Rhys factor *S* is used to describe the strength of electron-phonon coupling, and the electron-phonon coupling has a strong relationship with the FWHM of emission, meeting the following equation[11]

$$FWHM = 2.36\sqrt{S}\hbar\omega_{phonon}\sqrt{\coth\frac{\hbar\omega_{phonon}}{2k_BT}}$$

where $\hbar$ is reduced Planck constant, ω_{phonon} represents phonon frequency, T is temperature, and k_B Boltzmann constant.

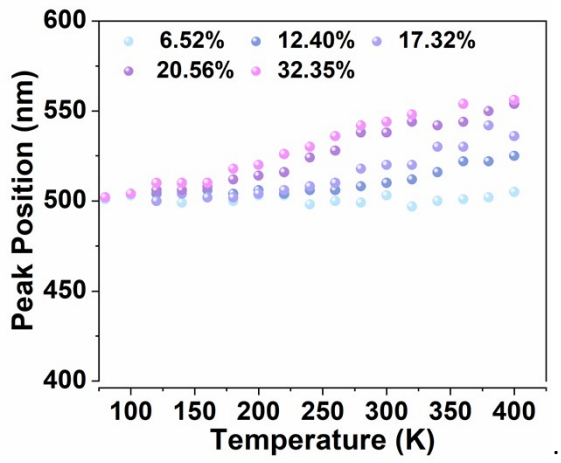

Fig. S19 Temperature-dependent peak position evolution of Ag-alloyed β-$Cs_3Cu_2Br_5$.

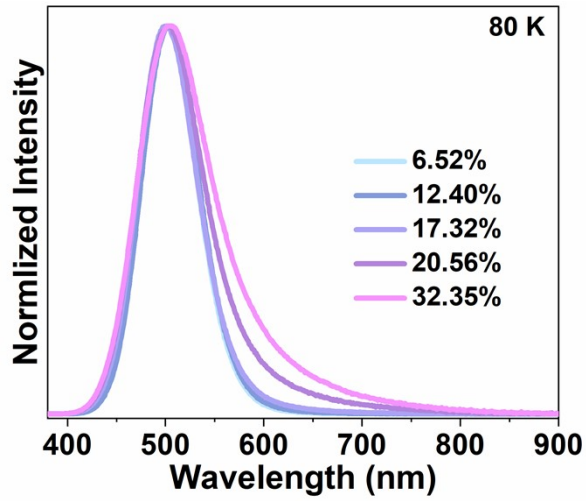

Fig. S20 PL spectra of Ag-alloyed β-$Cs_3Cu_2Br_5$ at 80 K.

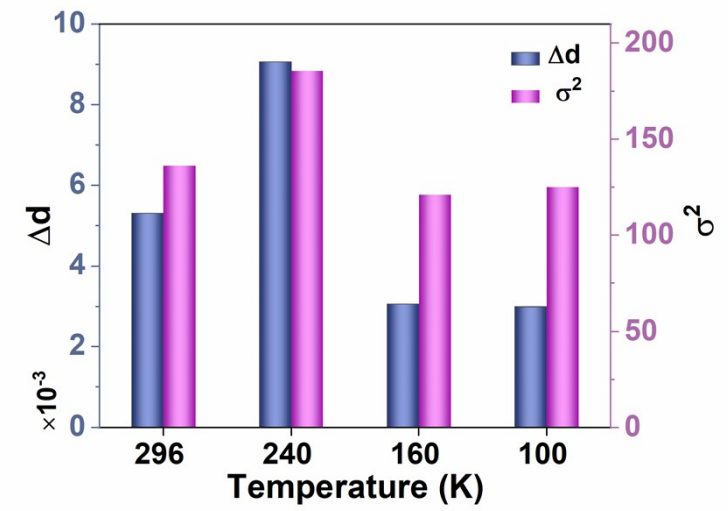

Fig. S21 Tetrahedral parameters of β-$Cs_3Cu_2Br_5$:32.35%Ag^+ at different temperature.

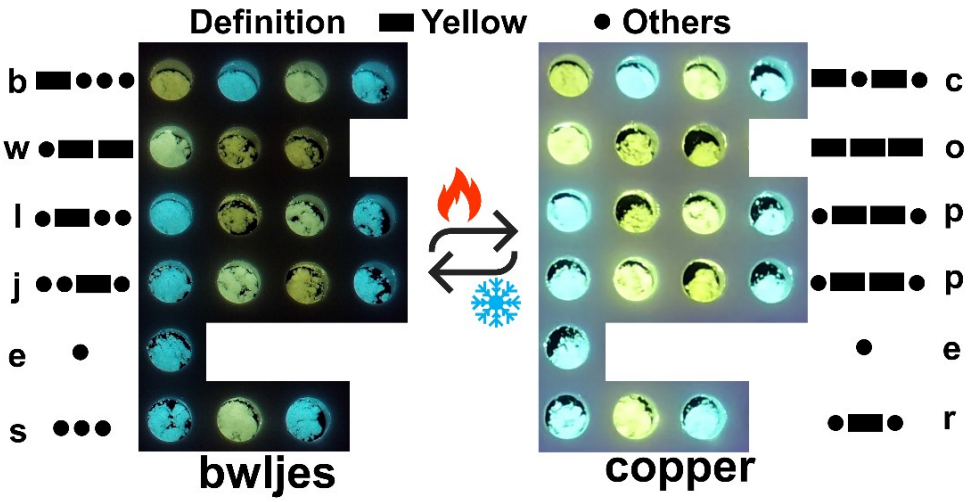

Fig. S22 Images of β-$Cs_3(Cu/Ag)_2Br_5$ based encryption and decryption patterns. The encryption word 'copper' shows wrong information as 'bwljes' under room temperature.

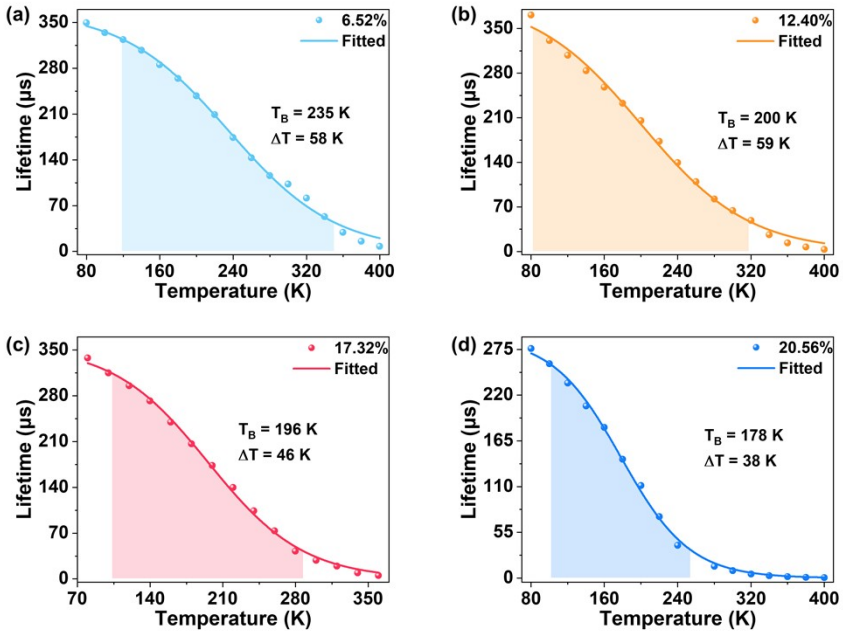

Fig. S23 Temperature dependence of lifetime in Ag-alloyed β-$Cs_3Cu_2Br_5$ samples. The filled color areas represent the sensing range.

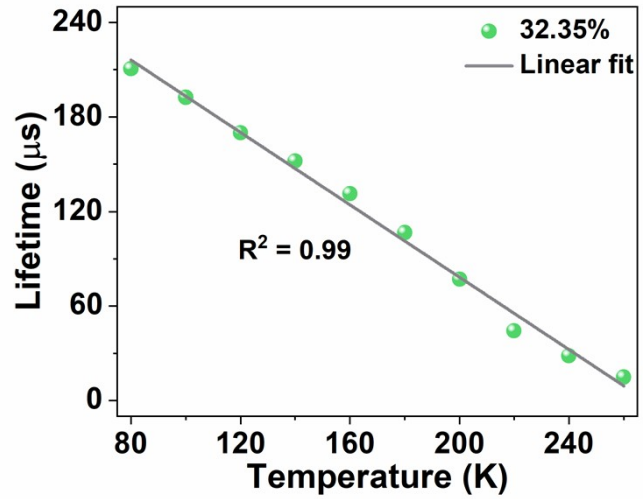

Fig. S24 Linear relationship between temperature and average lifetime of Ag-0.85 in the range of 80 to 260 K.

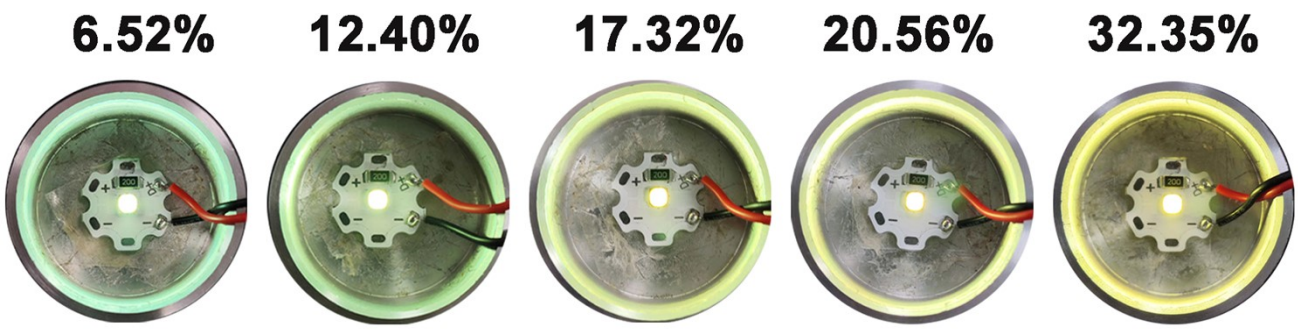

Fig. S25 Photograph of the fabricated LED device based on different β-$Cs_3Cu_2Br_5$:xAg^+ samples.

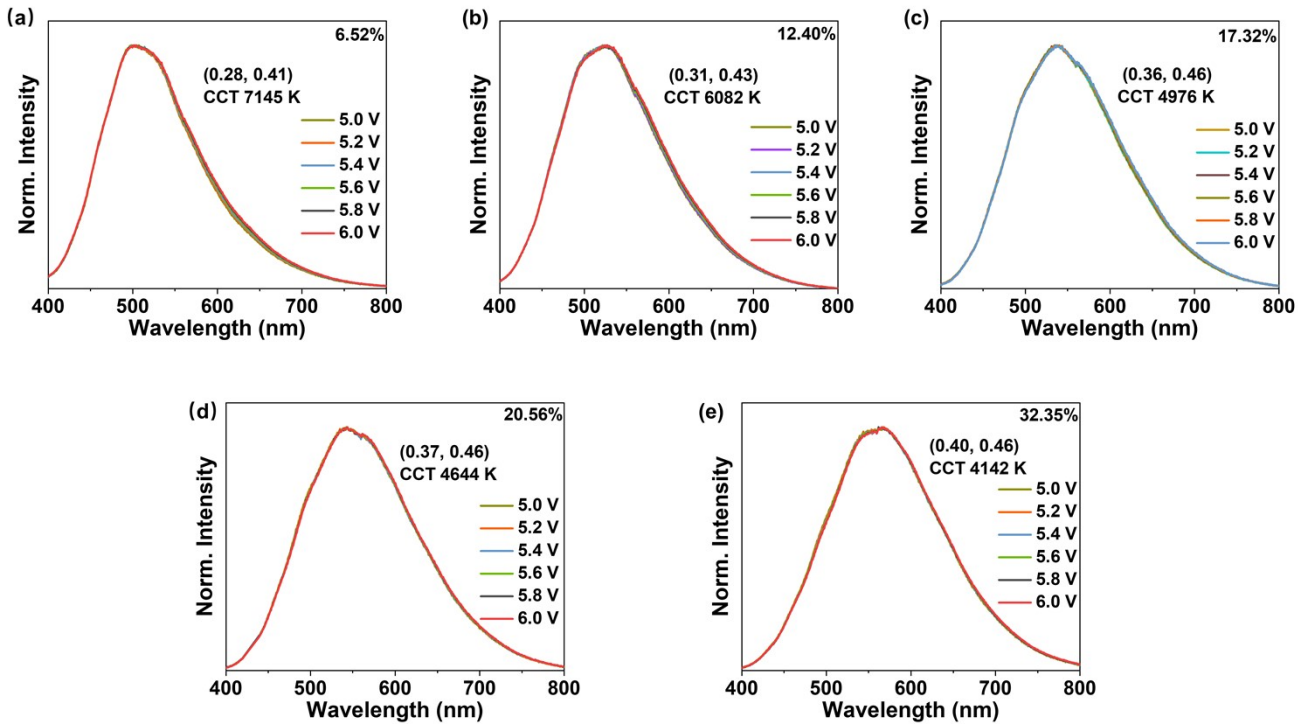

Fig. S26 EL spectra of fabricated LED device based on different β-$Cs_3Cu_2Br_5$:xAg^+ samples under different voltage.

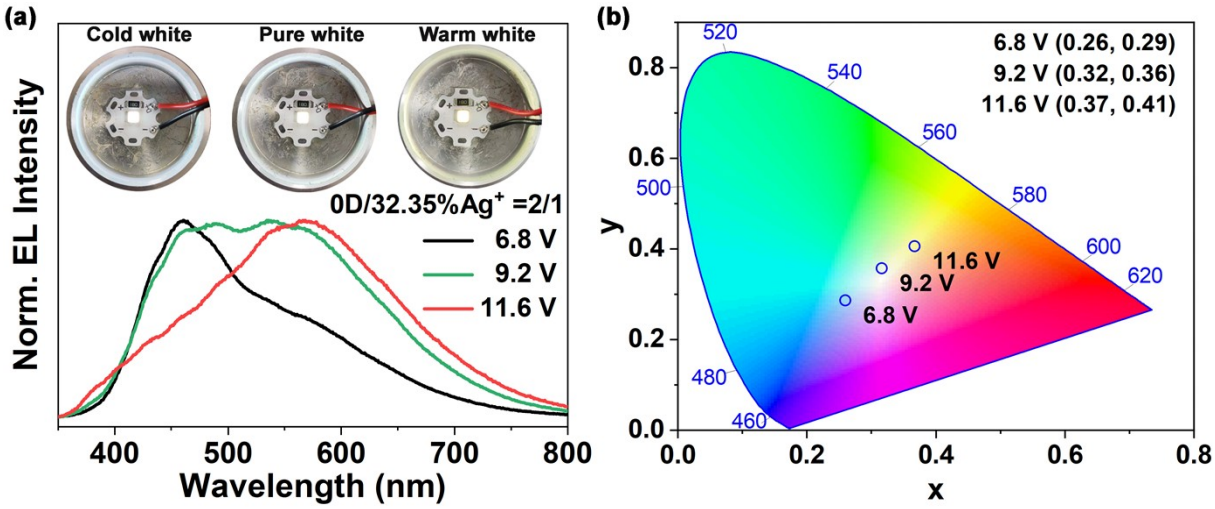

Fig. S27 (a) EL spectra and photograph of LED device based on a mixture of 0D and β-$Cs_3Cu_2Br_5$:32.35%Ag^+ samples with a mass ratio of 2:1 and a 275 nm UV LED chip under different voltage, and (b) the corresponding CIE color coordinate change.

Table S1. ICP-MS results of Ag and Cu in Ag-alloyed β-$Cs_3Cu_2Br_5$.

Sample	Ag (mg/L)	Cu (mg/L)	Ag/Cu ratio in feeding solution	Actual Ag/Cu ratio
Ag-0.11	2.5131	21.203	11%	6.52%
Ag-0.21	4.5771	19.048	21%	12.40%
Ag-0.43	9.5196	26.769	43%	17.32%
Ag-0.64	10.445	23.774	64%	20.56%
Ag-0.85	15.877	12.888	85%	32.35%

Table S2. Crystal data and structure refinement for Ag-0.11 and Ag-0.85.

Compound	$Cs_3Cu_2Br_5$ (β−$Cs_3Cu_2Br_5$:6.52%Ag^+)	$Cs_3Cu_{1.5}Ag_{0.5}Br_5$ (β−$Cs_3Cu_2Br_5$:32.35%Ag^+)
Formula weight (g·mol^{-1})	925.36	947.49
Temperature (K)	279	297
Crystal system	orthorhombic	orthorhombic
Space group	Cmcm (63)	Cmcm (63)
Cell parameters	a =16.2298(6) Å b = 9.1626(3) Å c = 9.0004(3) Å α, β, γ = 90°	a = 16.3496(6) Å b = 9.2138(3) Å c = 9.0533(3) Å α, β, γ = 90°
Volume ($Å^3$)	1338.42(8)	1363.81(8)
Z	2	16
Density (g·cml^{-3})	4.592	4.615
μ (mm^{-1})	26.090	25.543
F (000)	1228.0	1628.0
Theta max (°)	30.660	30.644
h, k, l_{max}	23, 12, 12	22, 13, 12
GOF.	1.106	1.094
Final R index	R_1 = 0.0388(942) wR_2 = 0.1046(1080)	R_1 = 0.0267 wR_2 = 0.0752

Table S3. The fitted results of the PL decay curves of Ag-alloyed β-$Cs_3Cu_2Br_5$: xAg^+.

Sample	Excitation wavelength	Monitoring wavelength	τ_1 (μs)	A_1	Rel_1%	τ_2 (μs)	A_2	Rel_2%	τ_{ave} (μs)
6.52%Ag^+	340 nm	502 nm	33.38	1371.84	8.56	149.19	3278.77	91.54	139.28
12.40%Ag^+	340 nm	508 nm	18.90	2250.22	16.99	90.22	2302.78	83.01	78.09
17.32%Ag^+	340 nm	526 nm	6.06	0.1456	27.78	45.92	0.0453	70.22	34.05
20.56%Ag^+	340 nm	537 nm	2.81	0.1185	54.16	19.92	0.0142	45.84	10.65
32.35%Ag^+	340 nm	545 nm	2.00	0.0368	61.61	12.60	0.0036	38.39	6.07

Table S4. The bond length and bond angle evolution of β-$Cs_3Cu_2Br_5$:xAg^+ (x = 12.40%, 17.32%, 20.56%, 32.35%), r_1 and r_2 corresponding to intratetrahedral and intertetrahedral Cu-Cu distance of $[Cu_2Br_6]^{4-}$ units, respectively.

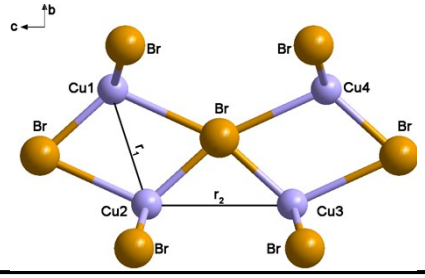

Bond length (Å)	12.40%	17.32%	20.56%	32.35%
Cu1 – Br1	2.4277	2.4293	2.4298	2.472
Cu1 – Br2	2.4714	2.9012	2.5221	2.508
Cu1 – Br3	2.9288	2.5385	2.4298	2.919
Cu1 – Br4	2.4277	2.4293	2.9810	2.472
r_1	2.9752	3.2327	3.1326	2.9742
r_2	3.6655	3.5857	3.6185	3.6974
Bond Angles (°)	**12.40%**	**17.32%**	**20.56%**	**32.35%**
Br1-Cu1-Br2	122.741	95.259	113.927	122.404
Br1-Cu1-Br3	113.839	113.065	124.977	94.361
Br1-Cu1-Br4	94.167	95.259	93.398	113.794
Br2-Cu1-Br3	113.839	112.691	113.927	94.361
Br2-Cu1-Br4	113.763	124.272	111.187	113.794
Br3-Cu1-Br4	94.167	112.691	93.398	114.039
Br-Br-Br	168.29	167.497	167.025	166.58

Table S5. The refinement crystal parameters of β-$Cs_3Cu_2Br_5$:32.35%Ag^+ under different temperatures.

Compound	$Cs_3Cu_{1.5}Ag_{0.5}Br_5$ (β-$Cs_3Cu_2Br_5$:32.35%Ag^+)			
Temperature (K)	297	240	160	100
Formula weight	947.49	947.49	947.49	947.49
Crystal system	orthorhombic	orthorhombic	orthorhombic	orthorhombic
Space group	Cmcm (63)	Cmcm (63)	Cmcm (63)	Cmcm (63)
Cell parameters	a = 16.3496(6) Å b = 9.2138(3) Å c = 9.0533(3) Å α, β, γ = 90°	a = 16.3094(4) Å b = 9.1770(2) Å c = 9.0242(3) Å α, β, γ = 90°	a = 16.2746(4) Å b = 9.1408(2) Å c = 8.9973(2) Å α, β, γ = 90°	a = 16.2466(4) Å b = 9.1132(2) Å c = 8.9796(2) Å α, β, γ = 90°
Volume ($Å^3$)	1363.81(8)	1350.66(6)	1338.46(5)	1329.51(5)
Z	16	16	16	16
Density ($g·cml^{-3}$)	4.615	4.660	4.702	4.734
μ (mm^{-1})	25.543	25.792	26.027	26.202
F (000)	1628.0	1628.0	1628.0	1628.0
Theta max (°)	30.644	30.660	30.660	30.660
h, k, lmax	22, 13, 12	23, 13, 12	22, 12, 12	22, 13, 12
GOF.	1.094	1.094	1.067	1.086
Final R index	R_1=0.0267 wR_2=0.0752	R_1=0.0311 wR_2=0.0838	R_1=0.0304 wR_2=0.0798	R_1=0.0274 wR_2=0.0714

Table S6. The fitted results of the PL decay curves at different temperture for β-$Cs_3Cu_2Br_5$:12.40%Ag^+.

Temperature (K)	τ_1 (μs)	rel_1%	τ_2 (μs)	rel_2%	τ_{ave} (μs)
80	8.73	1.85	378	98.15	371.2
100	5.38	2.13	338.4	97.87	331.3
120	7.049	2.37	315.3	97.63	308.0
140	19.20	2.82	291.6	97.18	283.9
160	23.57	3.45	266.5	96.55	258.1
180	23.21	4.32	242.4	95.68	232.9
200	18.81	5.7	216.7	94.30	205.4
220	21.78	7.4	185.1	92.60	173.0
240	21.24	9.62	152.1	90.38	139.5
260	20	12.56	122.7	87.44	109.8
280	19.23	15.97	94.68	84.03	82.63
300	17.90	19.72	75.88	80.28	64.45
320	14.84	21.36	57.87	78.64	48.68
340	5.79	19.9	31.7	80.10	26.55
360	3.574	22.13	16.19	77.87	13.4
380	2.34	24.22	8.76	75.78	7.2
400	1.34	31.60	4.36	68.40	3.40

Table S7. The fitted results of the PL decay curves of β-$Cs_3Cu_2Br_5$:x%Ag^+.

Sample	Temperature (K)	τ_1 (μs)	rel_1%	τ_2 (μs)	rel_2%	τ_3 (μs)	rel_3%	τ_{ave} (μs)
6.52%	80	26.51	1.67	355.4	98.33			349.9
	360	6.17	15.35	33.68	84.65			29.45
17.32%	80	13.87	4.08	351.9	95.92			338.1
	360	1.96	28.24	6.44	71.76			5.18
20.56%	80	4.66	8.7	58.73	14.54	347.9	76.76	276
	360	0.64	35.06	2.21	64.94			1.66
32.35%	80	4.44	11.88	46.53	18.68	290.2	69.44	210.7
	360	0.55	42.08	1.64	57.92			1.18

Table S8. Summary of the recent reports on traditional materials and metal halide-based thermometry.

Materials	Probe range (K)	α_{max} (K^{-1} %)	Ref.
YVO_4:YbTm	300-1009	2.13	S12
$[C(NH_2)_3]_2SnBr_4$	173-303	6.0	S13
$(C_9H_{15}N_3)ZnCl_4$: Mn^{2+}	110-290	0.57	S14
N,S-Carbon dots	275-353	1.79	S15
PbS QDs	150-350	1.3	S16
β-$Cs_3Cu_2Br_5$:6.52%Ag^+	119-351	1.6	This work
β-$Cs_3Cu_2Br_5$:32.35%Ag^+	102-246	2.8	This work

Table S9. Summary of LED device performance based on β-$Cs_3Cu_2Br_5$:x%Ag^+

Sample	EQE	CRI
β-$Cs_3Cu_2Br_5$:6.52%Ag^+	0.35%	69.51
β-$Cs_3Cu_2Br_5$:12.40%Ag^+	0.63%	70.35
β-$Cs_3Cu_2Br_5$:17.32%Ag^+	0.33%	70.62
β-$Cs_3Cu_2Br_5$:20.56%Ag^+	0.64%	71.63
β-$Cs_3Cu_2Br_5$:32.35%Ag^+	0.67%	74.2
0D $Cs_3Cu_2Br_5$ + 32.35%Ag^+	0.11%	83.49

SUPPORTING REFERENCES

1. Q. Li, Z. Chen, B. Yang, L. Tan, B. Xu, J. Han, Y. Zhao, J. Tang and Z. Quan, Pressure-Induced Remarkable Enhancement of Self-Trapped Exciton Emission in One-Dimensional $CsCu_2I_3$ with Tetrahedral Units, *J. Am. Chem. Soc.*, 2020, **142**, 1786-1791.
2. K. Robinson, G. V. Gibbs and P. H. Ribbe, Quadriatic Elongation-Quantitative Measure of Distortion in Coordination Polyhedra, *Science*, 1971, **172**, 567-570.
3. J. F. G. Kresse, Efficient Iterative Schemes for Ab Initio Total-Energy Calculations Using a Plane-Wave Basis Set, *Phys. Rev. B*, 1996, **54**, 11169-11186.
4. G. Kresse and J. Hafner, Ab Initiomolecular-Dynamics Simulation of the Liquid-Metal–Amorphous-Semiconductor Transition in Germanium, *Phys. Rev. B*, 1994, **49**, 14251-14269.
5. P. E. Blöchl, Projector Augmented-Wave Method, *Phys. Rev. B*, 1994, **50**, 17953-17979.
6. G. K. D. Joubert, From ultrasoft pseudopotentials to the projector augmented-wave method, *Phys. Rev. B* 1999, **59**, 1758-1775.
7. J. P. Perdew, K. Burke and M. Ernzerhof, Generalized Gradient Approximation Made Simple, *Phys. Rev. Lett.*, 1996, **77**, 3865-3868.
8. Y. Zhu, X. Y. Guo, L. N. Jiang, Z. R. Yan, Y. Yan and X. F. Han, Giant Tunneling Magnetoresistance in van der Waals Magnetic Tunnel Junctions Formed by Interlayer Antiferromagnetic Bilayer $CoBr_2$, *Phys. Rev. B*, 2021, **103**, 134437.
9. S. Froyen, Brillouin-Zone Integration by Fourier Quadrature: Special Points for Superlattice and Supercell Calculations, *Phys. Rev. B*, 1989, **39**, 3168-3172.

10. A. Yadav, Vikram, N. Singh and A. Alam, Mixed-Functionalized Sc_2CT_x (t=O, OH, F) Mxenefor Electrocatalytic CO_2 Reduction: Insight from First-Principles Calculations, *Phys. Rev. Appl.*, 2022, **18**, 024020.
11. S. Li, S. Li, J. Luo, J. Liu and J. Tang, Self-Trapped Excitons in All-Inorganic Halide Perovskites: Fundamentals, Status, and Potential Applications, The Journal of Physical Chemistry Letters, 2019, 10, 1999-2007. J. Luo, J. Liu and J. Tang, Self-Trapped Excitons in All-Inorganic Halide Perovskites: Fundamentals, Status, and Potential Applications, *J. Phys. Chem. Lett.*, 2019, **10**, 1999-2007.
12. M. Runowski, P. Wozny, N. Stopikowska, I. R. Martin, V. Lavin and S. Lis, Luminescent Nanothermometer Operating at Very High Temperature-Sensing up to 1000 K with Upconverting Nanoparticles (Yb^{3+}/Tm^{3+}), *ACS Appl. Mater. Interfaces*, 2020, **12**, 43933-43941.
13. S. Yakunin, B. M. Benin, Y. Shynkarenko, O. Nazarenko, M. I. Bodnarchuk, D. N. Dirin, C. Hofer, S. Cattaneo and M. V. Kovalenko, High-Resolution Remote Thermometry and Thermography Using Luminescent Low-Dimensional Tin-Halide Perovskites, *Nat. Mater.*, 2019, **18**, 846-852.
14. X. Zhang, Y. Xiong, K. Liu, N. Wang, L. Fan, W. Li, X. Zhao, J. Zhao and Q. Liu, Thermal Stable Zinc-Based Hybrid Halides with High External Quantum Efficiency as Temperature Detectors, *J. Mater. Chem. C*, 2022, **10**, 13137-13142.
15. S. Kalytchuk, K. Polakova, Y. Wang, J. P. Froning, K. Cepe, A. L. Rogach and R. Zboril, Carbon Dot Nanothermometry: Intracellular Photoluminescence Lifetime Thermal Sensing, *ACS Nano*, 2017, **11**, 1432-1442.
16. H. Zhao, A. Vomiero and F. Rosei, Ultrasensitive, Biocompatible, Self-Calibrating, Multiparametric Temperature Sensors, *Small*, 2015, **11**, 5741-5746.